Influence of Interfacial Energy on Electric-Field-Induced Sphere-to-Cylinder Transition in Block Copolymer Thin Films

Jia-Yu Wang, Wei Chen, and Thomas P. Russell*

Department of Polymer Science and Engineering, University of Massachusetts, Amherst, Massachusetts 01003

Received March 31, 2008; Revised Manuscript Received June 24, 2008

ABSTRACT: The effect of the interfacial energy on the electric-field-induced sphere-to-cylinder (S-to-C) transition in polystyrene-*b*-poly(methyl methacrylate) (PS-*b*-PMMA) copolymer thin films was studied as a function of the difference in the interfacial interactions of the PS and PMMA blocks with the substrate, δ. It was found that the interfacial energies altered both the critical electric field strength and the time scales of kinetics. A very strong preferential interfacial interaction suppressed the electric-field-induced S-to-C transition even though such a transition occurred on a neutralized surface where the interfacial interactions were balanced. For a moderate interfacial interaction, the S-to-C transition can be induced by an applied electric field, but the time scale of the morphology change is much longer. Furthermore, the formation of ionic complexes in the BCP was found to enhance the electric-field-induced S-to-C transition even on a native Si substrate without any surface modification, providing a simple route to generate ordered arrays of high-aspect-ratio cylinders oriented normal to a film surface.

Introduction

The self-assembly of block copolymers (BCPs) in thin films has attracted significant attention due to its potential application as templates and scaffolds for the fabrication of nanostructured materials.[1−4] Key for the successful implementation of this strategy is the control of the orientation and ordering of BCP microdomains. Electric fields have been proven to be an effective route to control the orientation of BCP microdomains in thin films.[5−8] The alignment arises from the difference in dielectric constants, $\Delta\varepsilon$, between two blocks.[9,10] Many studies have shown that the electric field can enhance fluctuations at the interface between the microdomains of the BCPs and align the lamellar and cylindrical microdomains in the direction of the applied field. This alignment is controlled by the applied electric field strength, the interfacial energies, $\Delta\varepsilon$, and the film thickness.[8,11−20] The interfacial energy of each block has proven to be an impediment in achieving complete alignment of the microdomains.[7,14,20] Specifically, to align the BCP microdomains normal to the film surface, the force resulting from the applied electric field has to be larger than a threshold value to overcome the preferential interfacial interaction that tend to align the BCP microdomains parallel to the substrate.

A dimensionless parameter δ, the absolute values of the relative difference in interfacial energies of each block with the substrate, is defined as $\delta = |\gamma_{AS} - \gamma_{BS}|/\gamma_T$, where γ_{AS} and γ_{BS} are the interfacial energies of block A and B with the substrate, respectively, and γ_T is the interfacial energy between block A and block B.[7] It describes the strength of the interfacial interactions and, hence, is a measurement of the force maintaining an orientation of the microdomains parallel to the substrate. Recently, Xu et al. reported that on a surface with the balanced interfacial interaction, $\delta = 0$, an electric field induced the sphere-to-cylinder (S-to-C) transition in BCP thin films.[21] The intermediate stages of this S-to-C transition showed that the spherical microdomains were initially deformed into ellipsoids by the applied electric field and subsequently interconnected into cylindrical microdomains oriented in the direction of electric field through the entire films. Several theoretical studies have appeared to describe this structure transition.[15,22−24] However, they do not discuss the influence of interfacial energy on the S-to-C transition and assume that the interfacial interactions are balanced.

On the other hand, Tsori et al.[22] proposed a "mobile ions mechanism" based on preliminary experimental observations of the S-to-C transition by Russell and co-workers and argued that the presence of the dissociated Li ions in the BCP could considerably lower the critical electric field strength for the S-to-C transition. Our recent experiments on the symmetric BCP thin films showed that uncomplexed Li ions had no effect on the electric-field-induced reorientation of the microdomains, whereas the complexed Li ions in the BCP could enhance alignment of lamellar microdomain due to the increase in $\Delta\varepsilon$, the difference in the dielectric constants between the blocks, and the mediation of the strong interfacial interactions.[26,27] Assuming that the results in the symmetric BCP copolymers are still applicable to the asymmetric BCP copolymers, to understand the effect of ionic complexes on the electric-field-induced S-to-C transition, it is necessary to know how the interfacial interactions affect this process.

Here, we investigate the effect of the interfacial energies on the electric-field-induced S-to-C transition in polystyrene-*b*-poly(methyl methacrylate) (PS-*b*-PMMA) copolymer thin films as a function of δ. Only when the interfacial interaction is balanced ($\delta = 0$), an electric-field-induced S-to-C transition occurs within a realistic time scale. Otherwise, the spherical microdomains are only elongated into ellipsoids with different stretching ratios. The studies of kinetics in S-to-C transition indicate that the interfacial energies alter both the critical electric field strength and the time scales of kinetics. We further provide evidence that the formation of ionic complexes in the BCP enhances the electric-field-induced S-to-C transition even on a native Si substrate without any surface modification. Consequently, the electric-field-induced S-to-C transition can be achieved by use of surfaces with balanced interfacial interactions or incorporating ionic complexes into the BCP.

Experimental Section

Materials. A deuterated polystyrene-*b*-deuterated poly(methyl methacrylate) (d-PS-*b*-d-PMMA) BCP used in this study was synthesized by sequential living anionic polymerization. The copolymer has a total number-average molecular weight $M_n = 128$

* To whom correspondence should be addressed. E-mail: russell@mail.pse.umass.edu.

10.1021/ma800717v CCC: $40.75
Published on Web 09/04/2008

kg/mol, a polydispersity PDI = 1.05, and a d-PS volume fraction $f_{d\text{-}PS}$ = 0.88. Although the deuteration of either block slightly changes the interaction between PS and PMMA blocks, it is not of significance to the studies presented here.[28]

Four hydroxyl-terminated random copolymers of styrene and methyl methacrylate with styrene fractions as 0.3 (30/70) 0.58 (58/42), 0.8 (80/20), and 0.9 (90/10) synthesized by living free radical polymerization were used to control the interfacial energies of each block with the substrates.[29] The random copolymers were covalently anchored to the surface, as described previously,[30] to give a ~6 nm copolymer brush. Using $\gamma_T = 0.8$ erg/cm^2, the values of δ are 0.53, 0, 0.73, and 0.94 respectively for styrene fractions of 0.30, 0.58, 0.8, and 0.9.[30−32]

Sample Preparation. Details on the substrate modification and measurement of the interfacial energy differences have been reported previously.[33] Neat block copolymer thin films were prepared by spin-coating the solutions of the copolymer in toluene onto either the native Si substrates or Si substrates modified by random copolymers.

The lithium-complexed d-PS-*b*-d-PMMA copolymer was made by mixing two solutions of lithium chloride (LiCl) in tetrahydrofuran (THF) and the copolymer in toluene at a given ratio with continuous stirring and moderate heating until most of THF was evaporated and the solutions became clear. Details about this process can be found in previous reports.[27,34] To ensure the formation of lithium complexes, the samples were measured by FT-IR and the percentage of the complexed carbonyl groups was estimated (see the Supporting Information). For the lithium-complexed d-PS-*b*-d-PMMA BCP, the thin films were prepared by spin-coating the mixed solutions onto the native Si substrates which preferentially interact with the d-PMMA block.

The electric field was applied across the thin films. All the electric-field experiments were performed at 170 °C under N_2 with field strength of ~40 V/μm for different periods of time and then quenched to room temperature before turning off the electric field. Samples for small-angle X-ray scattering (SAXS) measurements were prepared by drop-casting the mixed solutions onto Kapton films and then annealed at 170 °C under vacuum for 2 days. To prepare samples for transmission electron microscopy (TEM) measurements, a thin layer of carbon (~20 nm) was evaporated onto the surface of the samples before embedding into epoxy, which was cured at 60 °C overnight. The films were transferred from the substrate to the epoxy by dipping into liquid N_2. All samples were microtomed at room temperature with a diamond knife and then collected onto copper grids. The thin sections were exposed to ruthenium tetraoxide vapor for ~35 min to enhance the contrast.

Characterization. SAXS experiments were performed at room temperature under vacuum with the exposure time of 30−60 min, using an Osmic MaxFlux X-ray source with a wavelength λ of 1.54 Å and a 2-dimensional, multiwire proportional detector. The sample-to-detector distance (calibrated using silver behenate) was 1189 mm. TEM measurements were performed on a JEOL TEM200CX at an accelerating voltage of 200 kV. Tapping mode scanning force microscopy (SFM) measurements were performed with a Dimension 3000, Nanoscope III from Digital Instruments Corp. Grazing incidence small-angle X-ray scattering (GISAXS) measurements were performed at beamline X22B at National Synchrotron Light Source at Brookhaven National Laboratory using X-rays with a wavelength of λ = 1.5094 Å with an exposure time of 30 s per frame. Typical GISAXS patterns were taken at an incidence angle of 0.2°, above the critical angles of the copolymer and below the critical angle of the silicon substrate. Consequently, the entire structure of copolymer thin films could be detected.

Results and Discussion

Matsen calculated the relationship between the applied electric field strength, $\Delta\varepsilon$, and the volume fraction of the minor phase in BCPs and predicted that an optimum condition for the electric-field-induced S-to-C transition required a large dielectric contrast, a matrix composed of the low-dielectric constant material, and a BCP composition f as symmetric as possible.[23] On the basis of his argument, a d-PS-*b*-d-PMMA copolymer with M_w = 128K and $f_{d\text{-}PS}$ = 0.88 was used in this study. Figure 1 shows SAXS profile of the copolymer and the corresponding TEM image in the bulk after thermal annealing at 170 °C for 2 days. The SAXS profile for the neat copolymer shows two reflections at $1q^*$ and $5^{1/2}q^*$ (q^* is the value of q at the first peak and $q = (4\pi/\lambda)\sin(2\theta)$, where 2θ is the scattering angle), suggesting a spherical morphology.[35,36] The real-space observation by TEM further confirms the liquidlike packing of spherical microdomains (Figure 1b). Figure 1c is the TEM image of the top view of an ultrathin film with a thickness of ~35 nm on a native Si substrate after thermal annealing at 170 °C for 2 days. Hexagonal packed spherical microdomains are observed, verifying that the spherical microdomains are not be disrupted by the strong preferential interfacial interactions. The diameter of the d-PMMA microdomains is ~24 nm with a center-to-center distance of ~44 nm. In Figure 1d, the cross-sectional TEM image of a film with a thickness of ~600 nm on a native Si substrate after thermal annealing at 170 °C for 2 days demonstrates that the copolymer forms a spherical microdomain morphology, but the packing of multilayered spherical microdomains is not well-defined. All these results give evidence that the copolymers in both the bulk and thin films have a spherical microdomain morphology.

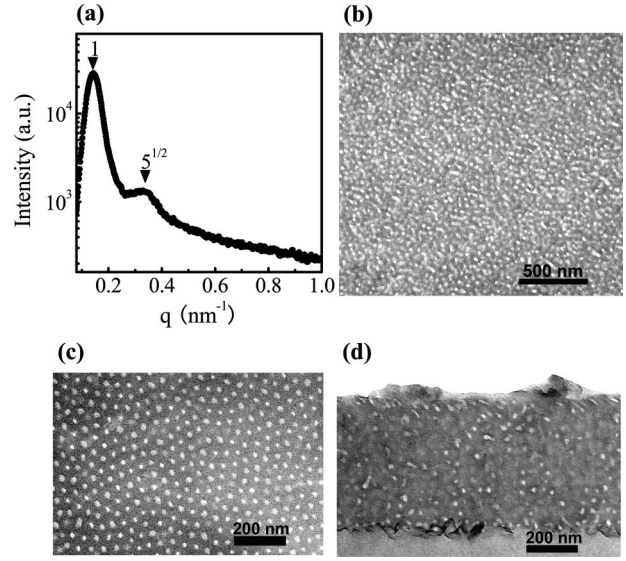

Figure 1. (a) SAXS profile and (b) TEM image of the d-PS-*b*-d-PMMA copolymer in the bulk after thermal annealing at 170 °C for 2 days followed by quenching to room temperature. (c) TEM image of a ~35 nm copolymer thin film and (d) cross-sectional TEM image of a ~600 nm copolymer thin film on the native Si substrate after thermal annealing at 170 °C for 2 days followed by quenching to room temperature.

The influence of the interfacial interactions on the electric-field-induced S-to-C transition was evaluated by use of the copolymer thin films on two different substrates. One was a native Si substrate that has a strong preferential interaction with PMMA block, and the other is a Si substrate on which the interfacial interactions are balanced by anchoring a 58/42 P(S-*r*-MMA) random copolymer. Shown in Figure 2 are the SFM phase images of these films after annealing under the applied electric field at 170 °C for 24 h. In contrast to a featureless SFM image for the film on the native Si substrate (Figure 2a), the hexagonal d-PMMA microdomains distributed in the d-PS matrix with the diameter of ~18 nm are observed for the film on the neutralized surface where the interfacial interactions are balanced (Figure 2b). The cross-sectional TEM image in Figure 2c shows that the multilayered spherical microdomains in the film on native Si

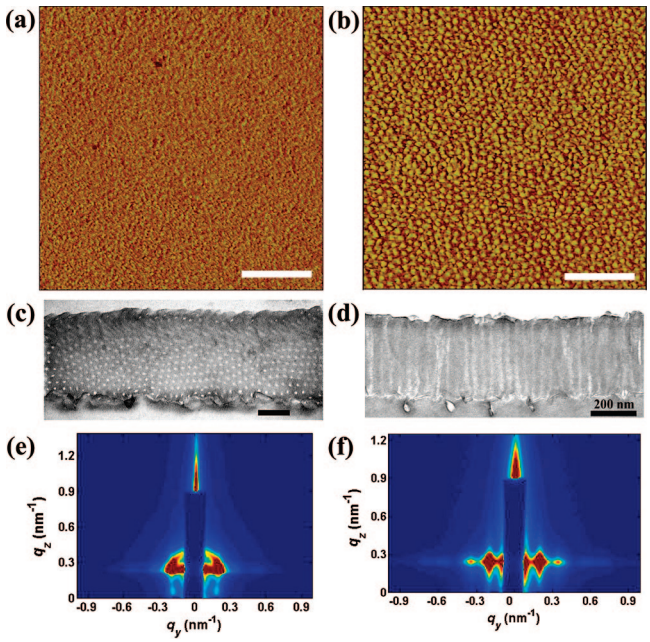

Figure 2. (a) SFM phase image of a ~600 nm d-PS-*b*-d-PMMA copolymer thin film on a native Si substrate after annealing at 170 °C under a ~40 V/μm electric dc field for 24 h. (c) The corresponding cross-sectional TEM image and (e) GISAXS pattern. (b) SFM phase image of a ~600 nm d-PS-*b*-d-PMMA copolymer thin film on a Si substrate modified by a P(S-*r*-MMA) random copolymer with a styrene fraction of 0.58 after annealing at 170 °C under a ~40 V/μm electric dc field for 24 h. (d) The corresponding cross-sectional TEM image and (f) GISAXS pattern. The interactions of the d-PS and d-PMMA blocks with this modified surface are balanced.[29] Scale bar in the SFM images is 500 nm, and scale bar in TEM images is 200 nm.

substrate are packed in a body-centered cubic lattice while in the film on the neutralized surface (Figure 2d), cylindrical microdomains oriented normal to the film surface penetrate through the entire film. The homogeneity of the structures over macroscopic lateral distances was further probed by GISAXS. The ring of scattering observed for the copolymer thin film prepared on the native silicon oxide substrate shows that the spherical microdomains are packed randomly (Figure 2e), whereas strong Bragg rods (vertical streaks) together with multiple higher-order reflections along the q_y direction are observed from the copolymer thin film on the neutralized surface (Figure 2f). The strong Bragg rods correspond to the first-order reflection from cylinders oriented normal to the surface with finite length. The multiple higher-order reflections with a ratio of peak positions of $1:3^{1/2}:2:7^{1/2}$ (q_y scan is not shown) indicate that cylindrical microdomains oriented normal to the substrate are laterally packed into hexagonal arrays, consistent with the SFM and cross-sectional TEM observations. Moreover, the absence of scattering along q_z direction indicates that there are no layered structures in the film. All these results suggest that interfacial energies play an important role in the electric-field-induced S-to-C transition. This is understandable since the spheres close to the substrate interface experience two opposing fields. The surface field tends to elongate spheres along the surface while the electric field tends to elongate spheres in the direction of the applied field. The competition between the surface and electric fields determines whether the spheres can be elongated in the direction of the applied electric field, and the final shape depends on the balance between the electrostatic pressure and surface tension. It has been predicted that an applied electric field less than the critical electric field strength for S-to-C transition cannot initiate the elongation of the spherical microdomains to form cylinders orientated in the direction of the electric field.[37] Here, the applied electric field

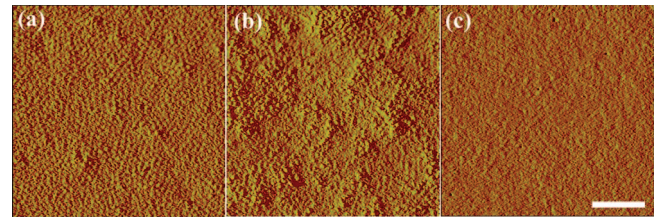

Figure 3. SFM phase images of the d-PS-*b*-d-PMMA copolymer thin films on the Si substrates modified by the P(S-*r*-MMA) random copolymers with a styrene fraction of (a) 0.3, (b) 0.8, and (c) 0.9 after annealing at 170 °C under a ~40 V/μm electric dc field for 24 h. Scale bar: 500 nm.

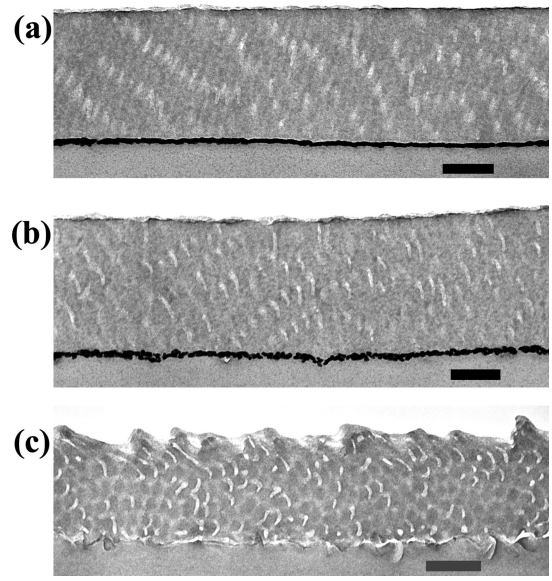

Figure 4. Cross-sectional TEM images of the d-PS-*b*-d-PMMA copolymer thin films on the Si substrates modified by the P(S-*r*-MMA) random copolymers with a styrene fraction of (a) 0.3, (b) 0.8, and (c) 0.9 after annealing at 170 °C under a ~40 V/μm electric dc field for 24 h. Scale bar: 200 nm.

cannot even deform the spheres into ellipsoids in the direction of the electric field for the film on the native silicon oxide substrate, indicating that the existence of strong preferential interfacial interactions significantly increases the critical electric field strength compared with the one on the neutralized surface.

The dependence of electric-field-induced S-to-C transition on the interfacial interactions was further examined as a function of δ. Figure 3 shows the SFM phase images of the copolymer thin films on the Si substrate modified by P(S-*r*-MMA) random copolymers with styrene fractions of 0.3, 0.8, and 0.9 after annealing at 170 °C under a ~40 V/μm electric dc field for 24 h. The corresponding δ values are 0.53, 0.73, and 0.94, respectively. For the copolymer film on the surface with δ = 0.53, the d-PMMA microdomains pack in hexagonal arrays with small areas of featureless defects (Figure 3a). As the strength of the interfacial interaction increases (δ = 0.73), the d-PMMA microdomains randomly distribute in a featureless matrix (Figure 3b). Further increasing the strength of the interfacial interaction to δ = 0.94, a completely featureless surface is observed (Figure 3c). The inner structures of these thin films examined by TEM are shown in Figure 4. For the film on the surface with δ = 0.53, short tilted cylindrical microdomains form. Lyakhova et al.[37] predicted that the interconnections of ellipsoids were not started in the electric field direction but rather dictated by the proximity of ellipsoids. The short cylinders formed would rotate as a whole by diffusion at a later stage and, eventually, orient normal to the substrate. According to this predication, the

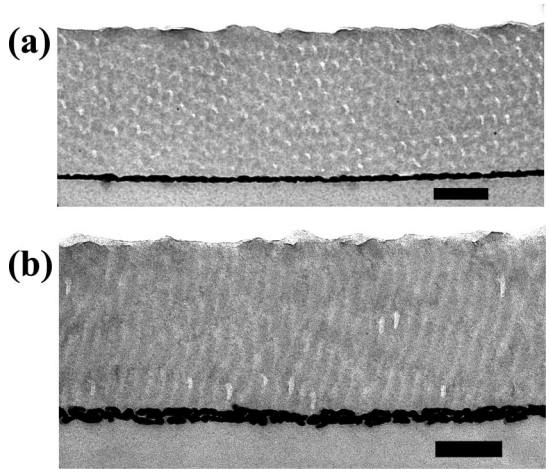

Figure 5. Cross-sectional TEM images of the d-PS-*b*-d-PMMA copolymer thin films on the Si substrates modified by a P(S-*r*-MMA) random copolymer with a styrene fraction of 0.8 after annealing at 170 °C under a ~40 V/μm electric dc field for (a) 5 h and (b) 48 h. Scale bar is 200 nm.

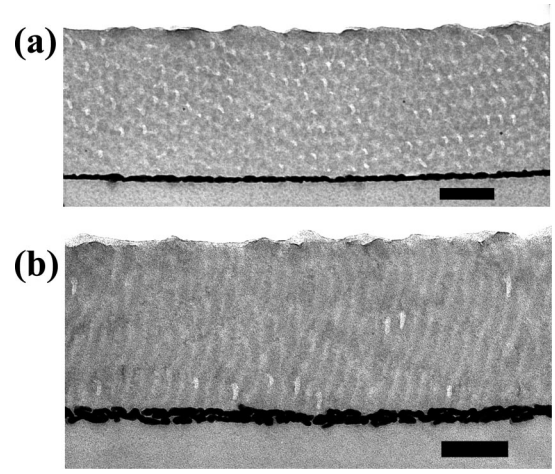

Figure 6. Cross-sectional TEM images of the d-PS-*b*-d-PMMA copolymer thin films on the Si substrate modified by a P(S-*r*-MMA) random copolymers with a styrene fraction of 0.58 after annealing at 170 °C under a ~40 V/μm electric dc field for (a) 5 h and (b) 18 h. Scale bar is 200 nm.

observation in Figure 4a indicates that the S-to-C transition is not a complete but an intermediate stage. Multilayers of short undulating cylinders are observed in the cross-sectional TEM image of the film on the surface with $\delta = 0.73$ (Figure 4b), indicating they are at the earlier intermediate stage of S-to-C transitions since the undulating cylinders are developed from the merge of elongated spheres in the films. Both elongated spheres and undulating short cylinders with the poor ordering coexist in the film on surface with $\delta = 0.94$, suggesting that this is at an even earlier stage of the S-to-C transition. Thus, the different stages of S-to-C transition occur at the same time scale in the films with different strengths of interfacial interactions, indicating that interfacial energies do have an effect on the kinetics of electric-field-induced S-to-C transition.

To further confirm the influence of interfacial energies on the kinetics of S-to-C transition, we compared the time evolution of the morphologies in thin films on surfaces with $\delta = 0.73$ and $\delta = 0$ at an earlier and later stage. Figure 5 is the cross-sectional TEM images of the copolymer thin films on the surface with $\delta = 0.73$ after annealing at 170 °C under a ~40 V/μm electric dc field for 5 and 48 h, respectively. For the film under the applied electric field for 5 h, the spherical microdomains have no deformation and seem identical to those in the film just after thermal annealing (Figure 1d). After annealing under the applied electric field for 48 h, the spherical microdomains have been converted into tilted cylindrical microdomains having different lengths. A similar structure evolution is observed in films where the interfacial interactions have been balanced. However, the time required for the transition is much shorter. Shown in Figure 6 are cross-sectional TEM images of the copolymer films on the neutralized surface after annealing at 170 °C under a ~40 V/μm electric dc field for 5 and 18 h. The spherical microdomains are already elongated along the electric field direction after annealing under the electric field for 5 h. These elongated spheres interconnect into short cylinders after annealing for 18 h (Figure 6b) and eventually transform into cylinders oriented normal to the substrate through the entire film after annealing for 24 h (Figure 2d). These results demonstrate that the electric-field-induced S-to-C transition is achievable for films on the surface with moderate interfacial interactions as long as the annealing times are long enough.

All the above results demonstrate the influence of interfacial energies on the electric-field-induced S-to-C transition. In our previous studies, it was shown that the formation of ionic complexes in PS-*b*-PMMA copolymers can increase $\Delta\varepsilon$ and

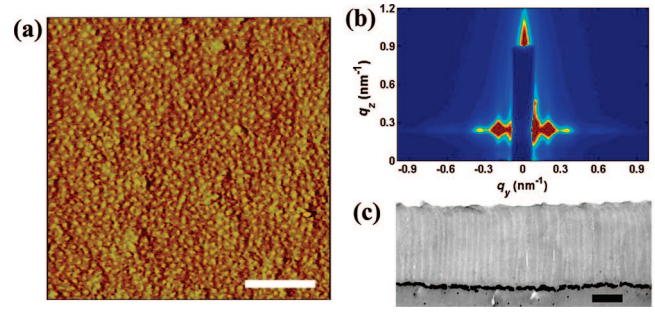

Figure 7. (a) SFM phase image of a ~500 nm thick film of d-PS-*b*-d-PMMA copolymer with ~4% of carbonyl groups coordinate to lithium ions on a native Si substrate after annealing at 170 °C under a ~40 V/μm electric dc field for 24 h. (b) The corresponding GISAXS pattern and (c) cross-sectional TEM image. Scale bar in SFM images is 500 nm, and scale bar in TEM images is 200 nm.

mediate the strong interfacial interactions at the substrate surface.[26,27] Here, the effect of ionic complexes on the electric-field-induced S-to-C transition was examined using the copolymer with ~4% of carbonyl groups coordinated to lithium ions. The complexed copolymer still exhibits a spherical microdomain morphology (see Supporting Information). Figure 7a is the SFM image of a ~500 nm thick film of this lithium-complexed copolymer on a native oxide substrate after annealing at 170 °C under a ~40 V/μm electric dc field for 24 h. Distinct from the neat copolymer film on the native Si substrate (Figure 2a), the hexagonal packing of the d-PMMA microdomains in the d-PS matrix is seen, similar to the neat copolymer film on a neutralized surface (Figure 2b). The inner structure of the film was further probed by GISAXS and cross-sectional TEM. In Figure 7b, the GISAXS pattern of strong Bragg rods (vertical streaks) together with multiple higher-order reflections along q_y give evidence that the cylindrical microdomains are oriented perpendicular to the substrate, consistent with the cross-sectional TEM result (Figure 7c). These results indicate that the formation of ionic complexes in the BCP enhances the electric-field-induced S-to-C transition in thin films.

The structure of lithium-complexed copolymer film at the early stage is shown in Figure 8. After annealing at 170 °C under a ~40 V/μm electric dc field for 5 h, spherical microdomains were elongated into ellipsoids with their long axes in the direction of the applied electric field. In contrast to the neat block copolymer film on a surface with balanced interfacial

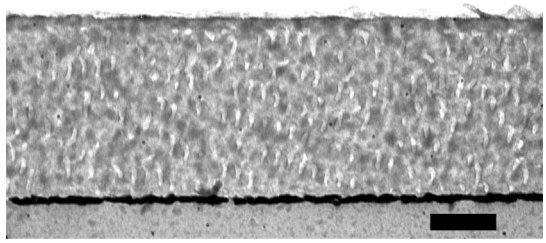

Figure 8. Cross-sectional TEM image of a thin film of the d-PS-*b*-d-PMMA copolymer with ~4% of carbonyl groups coordinate to lithium ions on a native Si substrate after annealing at 170 °C under a ~40 V/μm electric dc field for 5 h. Scale bar is 200 nm.

interaction after annealing for 5 h, the degree of stretching of the complexed copolymer is slightly higher, indicating that the kinetics of the ionic complexed copolymer film is more rapid than that of the neat copolymer.

Conclusions

We have shown that interfacial energies can affect the electric-field-induced S-to-C transition by increasing the critical electric field strength and prolonging the time scale of kinetics. A very strong preferential interfacial interaction can suppress the electric-field-induced S-to-C transition even though such transitions occurred on a neutralized surface under the same condition. For a moderate interfacial interaction, the S-to-C transition can be induced by an applied electric field, but the time scale of the morphology change is much longer. In addition, the formation of ionic complexes enhances the ability of the applied electric field to induce S-to-C transition due to a coupling of the increase of $\Delta\varepsilon$ and the mediation of interfacial interactions. By incorporation of ionic complexes into BCPs, the electric-field-induced S-to-C transition can be achieved without any surface modification, providing a simple route to generate the ordered arrays of high-aspect-ratio cylinders oriented normal to the surface.

Acknowledgment. This research was supported by the Department of Energy Basic Energy Science (DEFG0296ER45612) and the National Science Foundation-supported Material Research Science and Engineering Center at the University of Massachusetts, Amherst (DMR-0213695). We thank Dr. B. M. Ocko for the assistance with GISAXS experiments. Use of the National Synchrotron Light Source, Brookhaven National Laboratory, was supported by the U.S. Department of Energy, Office of Science, Office of Basic Energy Sciences, under Contract DE-AC02-98CH10886.

Supporting Information Available: FT-IR absorption spectrum of lithium-complexed d-PS-*b*-d-PMMA copolymers, SAXS profile, and the TEM images of the lithium-complexed d-PS-*b*-d-PMMA copolymer in the bulk and in thin films. This material is available free of charge via the Internet at http://pubs.acs.org.

References and Notes

(1) Hawker, C. J.; Russell, T. P. *MRS Bull.* **2005**, *30*, 952.
(2) Segalman, R. A. *Mater. Sci. Eng.* **2005**, *R48*, 191.
(3) Park, C.; Yoon, J.; Thomas, E. L. *Polymer* **2003**, *44*, 7779.
(4) Black, C. T.; Ruiz, R.; Breyta, G.; Cheng, J. Y.; Colburn, M. E.; Guarini, K. W.; Kim, H.-C.; Zhang, Y. *IBM J. Res. Dev.* **2007**, *51*, 605.
(5) Morkved, T. L.; Lu, M.; Urbas, A. M.; Ehrichs, E. E.; Jaeger, H. M.; Mansky, P.; Russell, T. P. *Science* **1996**, *273*, 931.
(6) Thurn-Albrecht, T.; Schotter, J.; Kastle, G. A.; Emley, N.; Shibauchi, T.; Krusin-Elbaum, L.; Guarini, K.; Black, C. T.; Tuominen, M. T.; Russell, T. P. *Science* **2000**, *290*, 2126.
(7) Tsori, Y.; Andelman, D. *Macromolecules* **2002**, *35*, 5161.
(8) Xu, T.; Zhu, Y.; Gido, S. P.; Russell, T. P. *Macromolecules* **2004**, *37*, 2625.
(9) Amundson, K.; Helfand, E.; Quan, X.; Smith, S. D. *Macromolecules* **1993**, *26*, 2698.
(10) Amundson, K.; Helfand, E.; Quan, X.; Hudson, S. D.; Smith, S. D. *Macromolecules* **1994**, *27*, 6559.
(11) Onuki, A.; Fukuda, J. *Macromolecules* **1995**, *28*, 8788.
(12) Kyrylyuk, A. V.; Zvelindovsky, A. V.; Sevink, G. J. A.; Fraaije, J. G. E. M. *Macromolecules* **2002**, *35*, 1473.
(13) Kyrylyuk, A. V.; Sevink, G. J. A.; Zvelindovsky, A. V.; Fraaije, J. G. E. M. *Macromol. Theory Simul.* **2003**, *12*, 508.
(14) Xu, T.; Hawker, C. J.; Russell, T. P. *Macromolecules* **2003**, *36*, 6178.
(15) Lin, C.-Y.; Schick, M.; Andelman, D. *Macromolecules* **2005**, *38*, 5766.
(16) Schmidt, K.; Boker, A.; Zettl, H.; Schubert, F.; Hansel, H.; Fischer, F.; Weiss, T. M.; Abetz, V.; Zvelindovsky, A. V.; Sevink, G. J. A.; Krausch, G. *Langmuir* **2005**, *21*, 11974.
(17) Xu, T.; Zvelindovsky, A. V.; Sevink, G. J. A.; Lyakhova, K. S.; Jinnai, H.; Russell, T. P. *Macromolecules* **2005**, *38*, 10788.
(18) Matsen, M. W. *Macromolecules* **2006**, *39*, 5512.
(19) Matsen, M. W. *Soft Mater.* **2006**, *2*, 1048.
(20) Pereira, G. G.; William, D. R. M. *Macromlecules* **1999**, *32*, 8115.
(21) Xu, T.; Zvelindovsky, A. V.; Sevink, G. J. A.; Gang, O.; Ocko, B.; Zhu, Y.; Gido, S. P.; Russell, T. P. *Macromolecules* **2004**, *37*, 6980.
(22) Tsori, Y.; Tournilhac, F.; Andelman, D.; Leibler, L. *Phys. Rev. Lett.* **2003**, *90*, 145504.
(23) Matsen, M. W. *J. Chem. Phys.* **2006**, *124*, 074906.
(24) Pinna, M.; Zvelindovskya, A. V.; Todd, S.; Goldbeck-Wood, G. *J. Chem. Phys.* **2006**, *125*, 154905.
(25) Tsori, Y.; Andelman, D.; Lin, C.-Y.; Schick, M. *Macromlecules* **2006**, *39*, 289.
(26) Wang, J.-Y.; Xu, T.; Leiston-Belanger, J. M.; Gupta, S.; Russell, T. P. *Phys. Rev. Lett.* **2006**, *96*, 128301.
(27) Wang, J.-Y.; Chen, W.; Sievert, J. D.; Russell, T. P. *Langmuir* **2008**, *24*, 3545.
(28) Russell, T. P.; Karis, T. E.; Gallot, Y.; Mayes, A. M. *Nature (London)* **1994**, *368*, 729.
(29) Hawker, C. J.; Elce, E.; Dao, J.; Volksen, W.; Russell, T. P.; Barclay, G. G. *Macromolecules* **1996**, *29*, 2686.
(30) Mansky, P.; Liu, Y.; Huang, E.; Russell, T. P.; Hawker, C. *Science* **1997**, *275*, 1458.
(31) Gates, B. D.; Xu, Q.; Stewart, M.; Ryan, D.; Willson, C. G.; Whitesides, G. M. *Chem. Rev.* **2005**, *105*, 1171.
(32) Gopalan, P.; Li, X.; Li, M.; Ober, C. K.; Gonzales, C. P.; Hawker, C. J. *J. Polym. Sci., Part A: Polym. Chem.* **2003**, *41*, 3640.
(33) Mansky, P.; Russell, T. P.; Hawker, C. J.; Mays, J.; Cook, D. S.; Satija, S. K. *Phys. Rev. Lett.* **1997**, *79*, 237.
(34) Wang, J.-Y.; Chen, W.; Roy, C.; Sievert, J. D.; Russell, T. P. *Macromolecules* **2008**, *41*, 963.
(35) Sakamoto, N.; Hashimoto, T.; Han, C. D.; Kim, D.; Vaidya, N. Y. *Macromolecules* **1997**, *30*, 1621.
(36) Kimishima, K.; Koga, T.; Hashimoto, T. *Macromolecules* **2000**, *33*, 968.
(37) Lyakhova, K. S.; Zvelindovsky, A. V.; Sevink, G. J. A. *Macromolecules* **2006**, *39*, 3024.

MA800717V